Wavelet and neuro-fuzzy conjunction model for predicting water table depth fluctuations

Ozgur Kisi and Jalal Shiri

ABSTRACT

The ability of a wavelet and neuro-fuzzy conjunction technique for groundwater depth forecasting was investigated in this study. The wavelet-neuro-fuzzy model was improved by combining two methods, the discrete wavelet transform and the neuro-fuzzy model. The conjunction model was applied to different input combinations of daily groundwater depth data of Bondville and Perry wells. Root mean square error (RMSE) and correlation coefficient (*R*) statistics were used for evaluating the accuracy of wavelet-neuro-fuzzy models. The accuracy of the conjunction models was compared with those of the single neuro-fuzzy models in one-, two- and three-day-ahead groundwater depth forecasting. Comparison of the results revealed that the wavelet-neuro-fuzzy models perform better than the neuro-fuzzy models especially for the two- and three-day-ahead forecasting cases.

Key words | forecasting, groundwater depth, neuro-fuzzy, wavelet-neuro-fuzzy

Ozgur Kisi
Engineering Faculty,
Civil Engineering Department, Hydraulics Divisions,
Erciyes University,
Kayseri,
Turkey

Jalal Shiri (corresponding author)
Water Engineering Department, Faculty of Agriculture,
University of Tabriz,
IR-51664 Tabriz,
Iran
E-mail: *j_shiri2005@yahoo.com*

INTRODUCTION

Groundwater is a significant source of drinking, domestic, industrial and irrigation water in the world, especially in arid and semi-arid areas where the precipitation is limited and fresh water is scarce. The knowledge of groundwater table fluctuations is of importance in agricultural lands, because it may be a limiting factor for some sensitive crops. To provide spatial and temporal information on aquifers and aquiferous systems and taking appropriate measures, studies related to groundwater levels are needed. Evaluation and prediction of groundwater levels through specific model(s) is required for forecasting and management of groundwater resources (Yang *et al.* 2005).

There are some empirical time series models such as described by Box & Jenkins (1976) and Hipel & McLeod (1994) to generate a longer time series of water table depths. Such empirical linear models have been widely used for water table depth modeling (Tankersley *et al.* 1993; Van Geer & Zuur 1997; Knotters & Van Walsum 1997). However, these models have their own limitations, because they are data demanding models and they are not adequate when the dynamical behavior of the hydrological system changes with time (Bierkens 1998). Moreover, the relationships between the precipitation, surface water and groundwater are generally nonlinear. However, solving non-linear equations is quite difficult and only few non-linear models such as stochastic differential equations and threshold autoregressive self-exciting models have been proposed for shallow water table modeling (Bierkens 1998; Knotters & De Gooijer 1999).

In this context, the use of artificial intelligence has received more attention in water resources engineering (Mukhopadhyay 1999; ASCE 2000a, b; Maier & Dany 2000; Minns & Hall 1996; Coulibaly *et al.* 2001; Beaudeau *et al.* 2001; Tayfur 2002; Cancelliere *et al.* 2002; Kumar *et al.* 2002; Supharatid 2003; Coppola *et al.* 2005a, b; Kisi 2006a, b, 2007; Szidarovszky *et al.* 2007; Coppola *et al.* 2007; Feng *et al.* 2008).

Recently, under artificial intelligence, effective data driving neuro-fuzzy models have attracted more attention due to their advantages. The adaptive neuro-fuzzy inference system

doi: 10.2166/nh.2012.104

(ANFIS) was first introduced by Jang (1993), Jang & Sun (1995), Jin *et al.* (1995), and later widely applied in engineering problems. Palit & Popovic (1999, 2000, 2005) applied neuro-fuzzy network for time-series forecasts. Deka & Chandramouli (2003) derived a river stage-discharge relationship using the fuzzy neural network model. Kisi (2005) estimated suspended sediment using neuro-fuzzy and neural network approaches. Kisi (2006c) proposed a neuro-fuzzy computing technique for daily pan evaporation modeling. Kisi & Ozturk (2007) used an adaptive neuro-fuzzy computing technique for evapotranspiration estimation. Aytek (2009) modeled evapotranspiration with a co-active neuro-fuzzy inference system. Moghaddamnia *et al.* (2009) applied neural networks and ANFIS techniques for evaporation estimation in a hot and dry climate in Iran.

In the last decade, wavelet transform has become a useful technique for analyzing variations, periodicities and trends in a time series (Smith *et al.* 1998; Lu 2002; Xingang *et al.* 2003; Coulibaly & Burn 2004; Labat 2005; Labat *et al.* 2005; Partal & Küçük 2006; Partal & Kisi 2007; Zhou *et al.* 2008; Wang *et al.* 2009; Milne *et al.* 2009; Shiri & Kisi 2010). Smith *et al.* (1998) used a discrete wavelet transform (DWT) for quantifying streamflow variability. They suggested that streamflows could be effectively classified into distinct hydroclimatic categories using DWT. Lu (2002) applied wavelet transform for the decomposition of interdecadal and interannual components of rainfall data in the rainy season. Xingang *et al.* (2003) investigated the rainfall spectrum and its evolution of North China in the rainy season with the summer monsoon decaying in interdecadal time scale using wavelet analysis. Coulibaly & Burn (2004) used wavelet analysis to identify and describe variability in annual Canadian streamflows and to gain insights into the dynamical link between the streamflows and the dominant modes of climate variability in the Northern Hemisphere. Labat (2005) reviewed the most recent wavelet applications in the field of earth sciences and illustrated new wavelet analysis methods (combined multiresolution-continuous wavelet analysis method, wavelet entropy) in the field of hydrology. Labat *et al.* (2005) demonstrated that the application of new wavelet indicators (combined continuous and multiresolution analysis, wavelet entropy, wavelet coherence, wavelet cross-correlation) leads to several improvements in the analysis of global hydrological signal (El Niño-Southern Oscillation, Southern Oscillation Index, North Atlantic Oscillation, South Atlantic Oscillation) fluctuations and of their mutual time-varying relationships. They concluded that wavelets should be used more systematically in preference to the classical Fourier analysis, notably in hydrology. Partal & Küçük (2006) used a DWT for determining the possible trends in annual total precipitation series. They used the precipitation records from meteorological stations in Turkey and concluded that the trend analysis on DWT components of the precipitation time series clearly explained the trend structure of data. All these studies showed that wavelet transform is an effective tool for precisely locating irregularly distributed multiscale features of climate elements in space and time. Partal & Kisi (2007) proposed a new conjunction model (wavelet-neuro-fuzzy) for precipitation forecast. They divided observed daily precipitations into some sub-series by using DWT and then used appropriate sub-series as inputs to the neuro-fuzzy models for forecasting daily precipitations. The wave-neuro-fuzzy model provided a good fit with the observed data. Zhou *et al.* (2008) proposed a wavelet predictor–corrector model for the simulation and prediction of the monthly discharge time series. First, they divided the monthly discharge time series into a certain number of detail signals and an approximated signal through wavelet transform. Then, they used ARMA model to predict each wavelet transform sub-series. After the stationary simulation prediction model of each series is obtained, the prediction results were superposed. Finally, they used an error autoregressive corrector model to correct the superposed prediction results. Wang *et al.* (2009) used a wavelet network model for predicting the inflows of the Three Gorges Dam on the Yangtze River and compared it with a threshold auto-regressive model (TAR). The results showed that the accuracy of the wavelet network model was generally better than the TAR model. Milne *et al.* (2009) investigated the temporal variation of river water solutes by using a wavelet packet transform. Shiri & Kisi (2010) used wavelet and neuro-fuzzy conjunction models for forecasting short- and long-term streamflows.

To the best knowledge of the authors the application of ANFIS and coupling wavelets with neuro-fuzzy is presented for the first time in this study for predicting groundwater depth fluctuations.

METHODS

Discrete wavelet transform

The wavelet function $\psi(t)$ called the mother wavelet, can be defined as $\int_{-\infty}^{+\infty} \psi(t)\,dt = 0$. Then $\psi_{a,b}(t)$ can be obtained through compressing and expanding $\psi(t)$:

$$\psi_{a,b}(t) = |a|^{-1/2}\psi\left(\frac{t-b}{a}\right) \quad b\,\varepsilon\,R,\ a\,\varepsilon\,R,\ a \neq 0 \tag{1}$$

where $\psi_{a,b}(t)$ = the successive wavelet, a = scale or frequency factor, b = a time factor; R = the domain of real numbers.

If $\psi_{a,b}(t)$ satisfies Equation (1), for the time series $f(t)\epsilon L^2(R)$ or finite energy signal, successive wavelet transform of $f(t)$ is defined as

$$W_\psi f(a,b) = |a|^{-1/2}\int_R f(t)\,\bar{\psi}\left(\frac{t-b}{a}\right)dt \tag{2}$$

where $\bar{\psi}(t)$ = complex conjugate functions of $\psi(t)$. It can be seen from Equation (2) that the wavelet transform is the decomposition of $f(t)$ under a different resolution level (scale). In other words, to filter the wave for $f(t)$ with a different filter is the essence of the wavelet transform.

The successive wavelet is often discrete in real applications. Let $a = a_0^j$, $b = kb_0a_0^j$, $a_0 > 1$, $b_0\ \epsilon\ R$, and k, j are integer numbers. Discrete wavelet transform of $f(t)$ can be written as

$$W_\psi f(j,k) = a_0^{-j/2}\int_R f(t)\,\bar{\psi}(a_0^{-j}t - kb_0)dt. \tag{3}$$

The most common (and simplest) choice for the parameters a_0 and b_0 is 2 and 1 time steps, respectively. This power of two logarithmic scaling of the time and scale is known as dyadic grid arrangement and is the simplest and most efficient case for practical purposes (Mallat 1989). Equation (3) becomes binary wavelet transform when $a_0 = 2$, $b_0 = 1$:

$$W_\psi f(j,k) = 2^{-j/2}\int_R f(t)\,\bar{\psi}(2^{-j}t - k)dt. \tag{4}$$

The characteristics of the original time series in frequency (a or j) and time domain (b or k) at the same time are reflected by $W_\psi f\,(a,b)$ or $W_\psi f\,(j,k)$. When the frequency resolution of wavelet transform is low, but the time domain resolution is high a or j becomes small. When the frequency resolution of wavelet transform is high, but the time domain resolution is low a or j becomes large (Wang & Ding 2003).

For a discrete time series $f(t)$, where it occurs at different time t (i.e. here integer time steps are used), the DWT can be defined as

$$W_\psi f(j,k) = 2^{-j/2}\sum_{t=0}^{N-1} f(t)\,\bar{\psi}(2^{-j}t - k) \tag{5}$$

where $W_\psi f\,(j,k)$ is the wavelet coefficient for the discrete wavelet of scale $a = 2^j$, $b = 2^jk$.

DWT operates two sets of functions viewed as high-pass and low-pass filters (see Figure 2). The original time series are passed through high-pass and low-pass filters and separated at different scales (Kisi 2009). The time series is decomposed into one comprising its trend (the approximation) and one comprising high frequencies and fast events (the detail). In the present study, the detail coefficients and approximation sub-time series are obtained by using Equation (5).

Adaptive neuro-fuzzy inference system

An ANFIS is a combination of an adaptive neural network (ANN) and a fuzzy inference system. The parameters of the fuzzy inference system are determined by the neural network learning algorithms. Since this system is based on the fuzzy inference system, reflecting amazing knowledge, an important aspect is that the system should be always interpretable in terms of fuzzy IF-THEN rules. ANFIS is capable of approximating any real continuous function on a compact set of parameters to any degree of accuracy (Jang *et al.* 1997). ANFIS identifies a set of parameters through a hybrid learning rule combining back propagation gradient descent error digestion and a least squared error method. There are mainly two approaches for fuzzy inference systems, namely the approaches of Mamdani (Mamdani & Assilian 1975) and Sugeno (Takagi & Sugeno 1985). The differences between the two approaches arise from the fact that Mamdani's approach uses fuzzy membership functions, while linear or constant functions are used in

Sugeno's approach. In this study the Sugeno method was applied for modeling the groundwater depth fluctuations.

ANFIS architecture

As a simple example a fuzzy inference system with two inputs x and y and one output z is assumed. Here, x and y might be considered as water table depths, h_{t-1} and h_{t-2}, in the $(t-1)$th and $(t-2)$th time steps respectively, while the output z would represent the water table depth at time t (h_t). Suppose that the rule base contains two fuzzy IF–THEN rules:

$$\text{Rule 1 : IF } x \text{ is } A_1 \text{ and } y \text{ is } B_1, \text{ THEN } f_1 = p_1 x + q_1 y + r_1 \quad (6)$$

$$\text{Rule 2 : IF } x \text{ is } A_2 \text{ and } y \text{ is } B_2, \text{ THEN } f_2 = p_2 x + q_2 y + r_2 \quad (7)$$

The IF (antecedent) part is fuzzy in nature, while the THEN (consequent) part is a crisp function of an antecedent variable (as a rule, a linear equation). For the study presented here for groundwater table, for the above example Equations (1) and (2) can be written as:

Rule 1 : IF h_{t-1} is LOW and h_{t-2} is LOW,
THEN $h_t = p_1 h_{t-1} + q_1 h_{t-2} + r_1$

Rule 2 : IF h_{t-1} is HIGH and h_{t-2} is MEDIUM,
THEN $h_t = p_2 h_{t-1} + q_2 h_{t-2} + r_2$

where p_i, q_i and r_i are parameters with $i = 1, 2, 3, \ldots, n$ corresponding to Rule 1, Rule 2, Rule 3, …, Rule n. The resulting type 3 Sugeno fuzzy reasoning model is shown in Figure 1. In a type 3 Sugeno fuzzy model, the output of each rule is a linear combination of input variables plus a constant term and the final output z is the weighted average of each rule output. The corresponding equivalent ANFIS architecture is represented in Figure 2. The node function in the same layer of the same function family, is described as follows (Jang 1993).

Layer 1

Every node i in this layer is an adaptive node with node function

$$O_i^l = \mu A_i(h_{t-1}) \quad (8)$$

where h_{t-1} is the input to the i-th node and A_i is a linguistic label (such as HIGH or LOW) associated with this node function. A similar equation as Equation (3) may be considered for the input h_{t-2}.

The node function O_i^l is the membership function of A_i and specifies the degree to which the given input h_{t-1} (or h_{t-2}) satisfies the quantifier A_i. The membership function for A is usually described by bell functions,

$$\mu A_i(h_{t-1}) = \frac{1}{1 + [(h_{t-1} - c_i)/a_i]^{2b_i}} \quad (9)$$

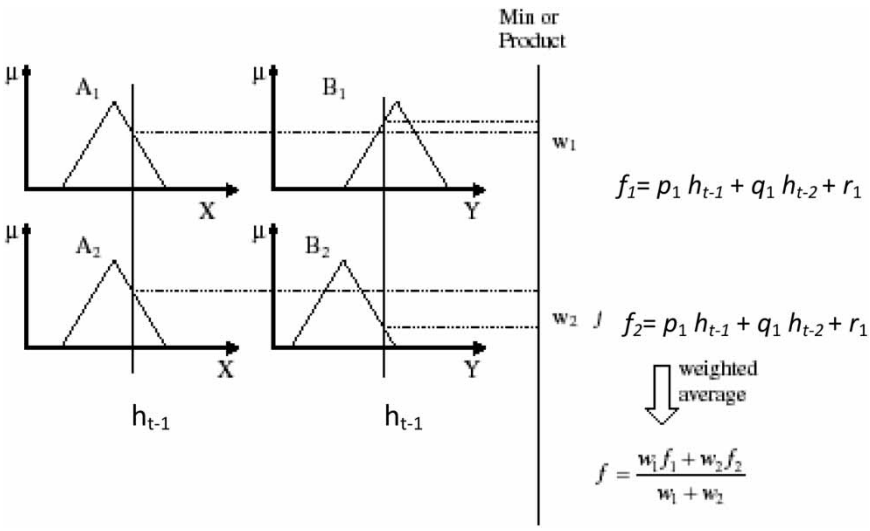

Figure 1 | Two input type-3 Sugeno fuzzy model with two rules.

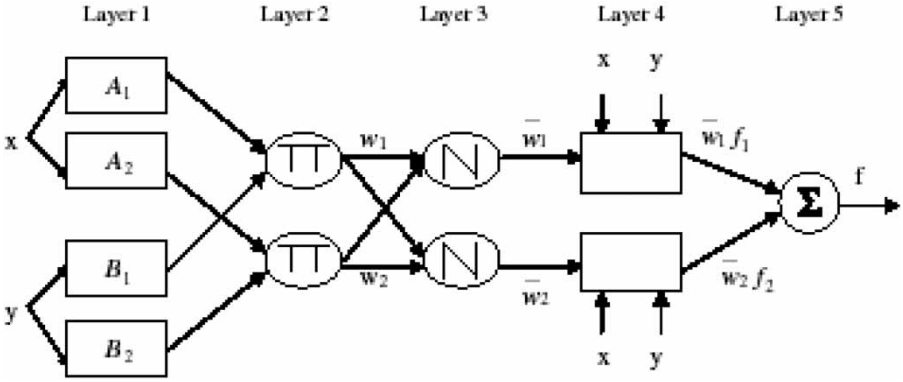

Figure 2 | Equivalent ANFIS architecture.

where $\{a_i, b_i, c_i\}$ is the parameter set and μ is the membership function of A_i. As the values of these parameters change, the bell-shaped function varies accordingly, thus exhibiting various forms of membership functions depending on the linguistic label A_i. In fact, any continuous and piecewise differentiable functions, such as commonly used triangular of trapezoidal membership functions, are also qualified candidates for node function in this layer. Parameters in this layer are referred to as *premise parameters*.

Layer 2

This layer consists of circle nodes labeled TT which multiply incoming signals and sending the product out. For instance

$$O_i^2 = w_i = \mu A_i(h_{t-1})\mu B_i(h_{t-2}), \quad i = 1, 2. \tag{10}$$

Each node output represents the firing strength of a rule.

Layer 3

In this layer, the circle nodes labeled *N*, calculate the ratio of the *i*th rule firing strength to the sum of all rule firing strengths

$$O_i^3 = \bar{w}_i \frac{w_i}{w_1 + w_2}, \quad \text{for } i = 1, 2. \tag{11}$$

The outputs of this layer are referred to as *normalized firing strengths*.

Layer 4

All of the nodes in this layer are adaptive with a node function

$$O_i^4 = \bar{w}_i f_i = \bar{w}_i(p_i h_{t-1} + q_i h_{t-2} + r_i) \tag{12}$$

where $\bar{w}_i$ is the output of layer 3, and $\{p_i, q_i, r_i\}$ is the parameter set. Parameters in this layer are called *consequence parameters*.

Layer 5

The single circle node of this layer, labeled Σ, computes the overall outputs as the summation of all incoming signals:

$$O_i^5 = \frac{\sum_i w_i \cdot f_i}{\sum_i w_i} \tag{13}$$

Thus an adaptive network which is functionally equivalent to a type 3 fuzzy inference system, has been constructed. More information about ANFIS theory can be found in, for example, Jang (1993) and Jang *et al.* (1997).

In the implementation of fuzzy logic, several types of membership functions can be used. However, recent studies have shown that the type of membership function does not affect the results fundamentally (Vernieuwe *et al.* 2005). In the present study, the triangular membership functions were used. The number of membership functions was determined by trial and error.

In the present work, firstly the single ANFIS model was studied to forecast groundwater table depth in two wells. Then, a conjunction model (wavelet-neuro-fuzzy) was applied for the same scope. The groundwater depth data considered were decomposed into a wavelet sub-series by DWT and the neuro-fuzzy model was constructed with appropriate wavelet sub-series as input and original water table depth time series as output. Finally, the performance of the hybrid wavelet-neuro-fuzzy model was compared with the classical neuro-fuzzy model.

APPLICATION

Data used

The dataset used in this study was obtained from the U.S. Illinois State Water Survey. The time series of daily depth to water table records from two wells are used; Bondville (station no: 421832, FIPS code: 019) and Perry (station no: 421843, FIPS Code: 149). The water table data of 1 September 2001 to 30 August 2008 were applied for training and testing ANFIS models. For each well, the first five years' data were used to train the models and the remaining data were used for testing. The periods from which training and testing data were chosen span the same temporal seasons (September–August). The daily statistical parameters of the water table data are given in Table 1. In the table, the X_{mean}, X_{max}, X_{min}, S_d, C_v and C_{sx} denote the mean, maximum, minimum, standard deviation, coefficient of variation and skewness, respectively. The skewness, a characterization of the degree of asymmetry of the distribution around the mean, is high for Perry well, particularly for the testing data. In the training data, X_{min} and X_{max} values fall in the ranges 0.37–9.89 m for Bondville well. However, the testing data set extremes are $X_{min} = 0.06$ m and $X_{max} = 9.81$ m. The value of X_{min} for the training data is higher than that for the corresponding testing set for Bondville well. This may cause extrapolation difficulties in estimation of low depth values.

Goodness of fit of model performance

Three statistical evaluation criteria were used to assess the model performance: (1) the coefficient of determination (R^2); (2) the RMSE defined as

$$\mathrm{RMSE} = \sqrt{\frac{1}{n}\sum_{i=1}^{n}(h_{io} - h_{ie})^2} \quad (14)$$

where h_{io} and h_{ie} denote the observed and estimated water table depths.

RESULTS AND DISCUSSION

The paper aims at representation of one-day-, two-day- and three-day-ahead forecasting of groundwater table fluctuations by ANFIS and Wavelet-ANFIS conjunction model. The Wavelet-ANFIS models were obtained by combining the two methods, DWT and ANFIS. The Wavelet-ANFIS is an ANFIS model which uses sub-time series components obtained using DWT on original data. For the Wavelet-ANFIS model inputs, the original time series are decomposed into a certain number of sub-time series components (Ds) by Mallat's DWT algorithm (Mallat 1989). Each component plays different role in the original time series and the behavior of each sub-time series is distinct (Wang & Ding 2003). The Wavelet-ANFIS is constructed in which

Table 1 | The daily statistical parameters of each well data set

		Statistical parameter					
Data set	**Well**	X_{mean} (m)	X_{max} (m)	X_{min} (m)	S_d (m)	C_v	C_{sx}
Training	Bondville (421832)	5.04	9.89	0.37	2.28	0.45	0.16
	Perry (421843)	9.02	21.38	0.04	6.01	0.66	0.49
Testing	Bondville (421832)	4.75	9.81	0.06	2.56	0.54	0.34
	Perry (421843)	8.63	19.52	0.24	6.30	0.73	0.65

the Ds of original input time series are input of the ANFIS and the original output time series are output of the ANFIS. It is relevant to note here that there are two sets of results considered in this section. Set 1 was produced in the course of the present study, where the Wavelet-ANFIS methodology was used. Set 2 was produced by Shiri & Kisi (2011) by applying ANFIS to the same training and testing combinations.

In the study, the current and previous groundwater depth time series were decomposed into various Ds at different resolution levels by using DWT to estimate one-day-, two-day- and three-day-ahead groundwater depth values. The original groundwater depth input time series of Bondville and Perry wells and their Ds, that is, the time series of two-day mode (D1), four-day mode (D2), eight-day mode (D3) and approximate mode are shown in Figures 3 and 4. The approximate mode indicates the trend (low frequency) of the original groundwater depth time series. It is obviously seen that the approximation series are very similar to the original groundwater depth time series.

The correlation coefficients between each D sub-time series and original daily groundwater depth time series are given in Table 2 for the Bondville and Perry wells, respectively. In this table, the D_t and GW_{t+1} denotes the D sub-time series at time t and measured groundwater depth at time $t+1$, respectively. As an example, the -0.016 shows the correlation value between D1 sub-time series at time t ($D1_t$) and measured groundwater depth at time $t+1$, GW_{t+1}. Thus, the $D1_t$, $D2_t \ldots$ denote the sub-time series of the GW_t and vice versa. The correlation values given in Table 2 provide information for the determination of effective wavelet components on groundwater depth. It can be seen from Table 2 that the D1, D2 and detail components show significantly low correlations for both wells. The approximate component has the highest correlations. According to these correlation analyses between Ds and original current groundwater depth data (output), the effective component (approximate component) was selected. For the Wavelet-ANFIS model, the new series obtained by using the approximation component was used as inputs to the ANFIS model.

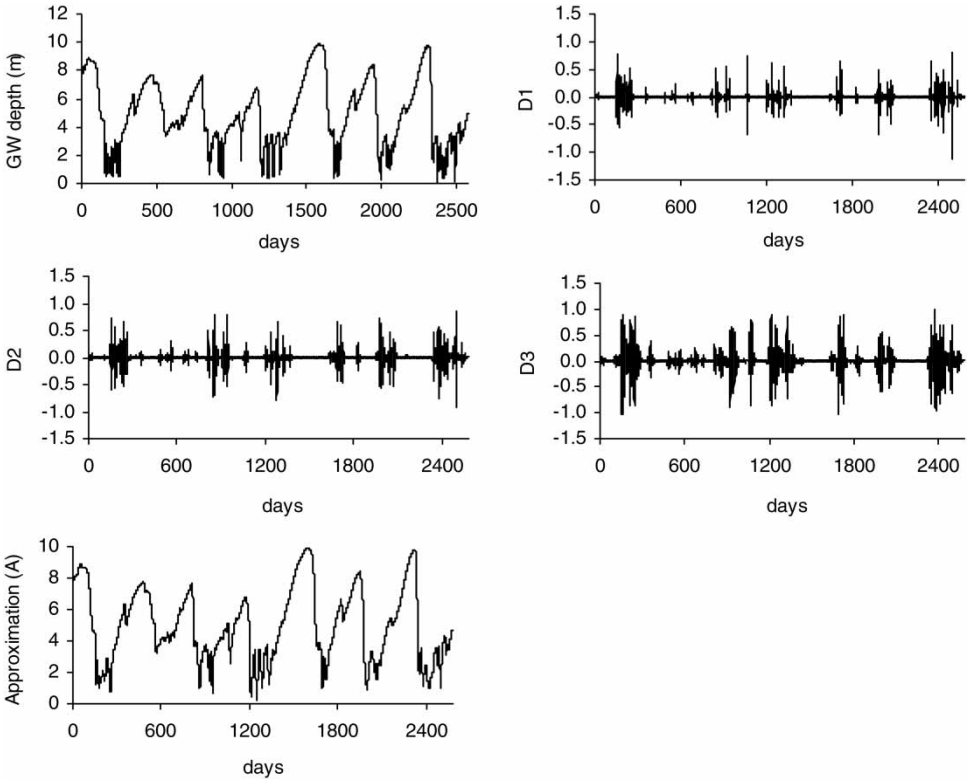

Figure 3 | Decomposed wavelet sub-time series components (Ds) of groundwater (GW) depth data of Bondville well.

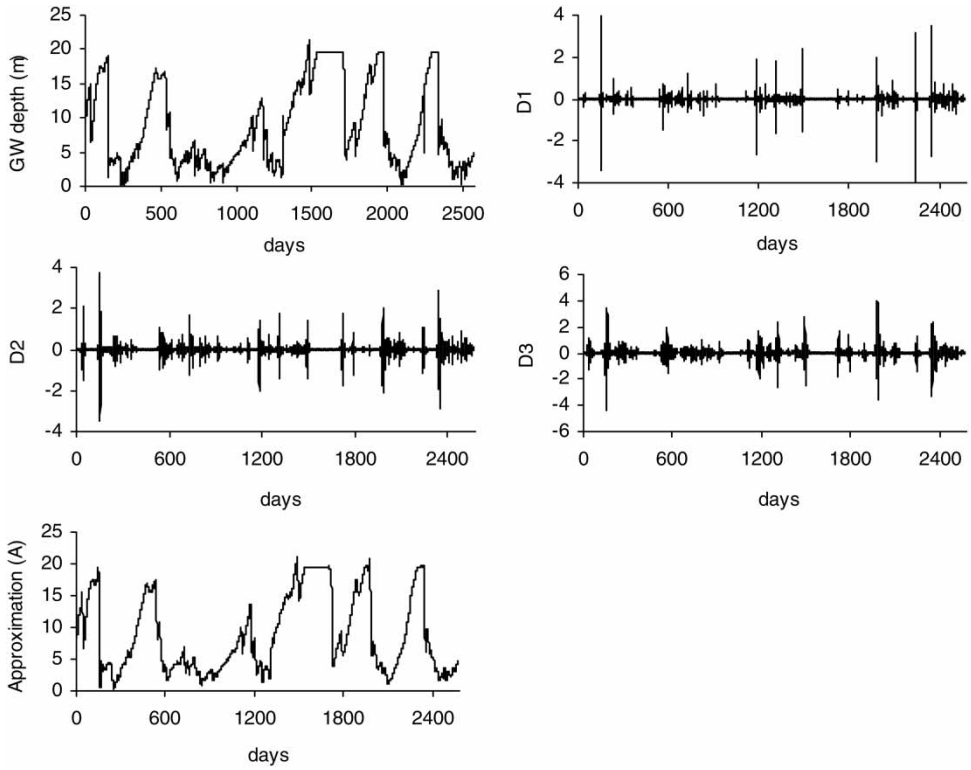

Figure 4 | Decomposed wavelet sub-time series components (Ds) of groundwater (GW) depth data of Perry well.

Table 2 | The correlation coefficients between each of sub-time series and original ground water depth

Discrete wavelet components	Correlations D_t/ GW_{t+1}	D_{t-1}/ GW_{t+1}	D_{t-2}/ GW_{t+1}	D_{t-3}/ GW_{t+1}	D_{t-4}/ GW_{t+1}
Bondville					
D1	–0.016	–0.011	0.008	0.007	–0.005
D2	0.027	–0.022	–0.040	–0.019	0.006
D3	0.069	0.034	–0.006	–0.041	–0.062
Approximate	0.993	0.990	0.986	0.979	0.971
Perry					
D1	–0.019	–0.008	0.006	0.003	–0.001
D2	0.029	–0.029	–0.044	–0.022	0.001
D3	0.063	0.037	0.006	–0.028	–0.051
Approximate	0.993	0.991	0.987	0.981	0.966

Shiri & Kisi (2011) applied several input combinations using ANFIS to estimate the water table depth for two wells. The inputs present the previous daily water table depths (t, $t-1, \ldots, t-5$) and the output layer node corresponds to the water table depth at time $t+1$, $t+2$ and $t+3$. Thus, the following combinations of input data of water table depth were evaluated:

(i) GW_t
(ii) GW_{t-1}, GW_t
(iii) GW_{t-2}, GW_{t-1}, GW_t
(iv) GW_{t-3}, GW_{t-2}, GW_{t-1}, GW_t
(v) GW_{t-4}, GW_{t-3}, GW_{t-2}, GW_{t-1}, GW_t .

Shiri & Kisi (2011) applied commonly used 'forward-stepwise selection of inputs' method (under a heuristic approach category) for selecting the appropriate input combinations. Forward selection is the more commonly used approach and begins by finding the best single input and selecting it for the final model (Bowden *et al.* 2005). In subsequent steps, different input variables are added into the input combination to evaluate the degree of the effect of each variable on output.

The final architectures of the ANFIS models for Bondville and Perry wells are given in Table 3. In the table,

Table 3 | The final architecture of the ANFIS models

Model inputs	The number of membership functions	
(i)	GW_t	3
(ii)	GW_{t-1}, GW_t	3 and 3
(iii)	GW_{t-2}, GW_{t-1}, GW_t	3, 2 and 3
(iv)	GW_{t-3}, GW_{t-2}, GW_{t-1}, GW_t	3, 3, 2 and 4
(v)	GW_{t-4}, GW_{t-3}, GW_{t-2}, GW_{t-1}, GW_t	2, 3, 3, 4 and 3

GW_i denotes the water table depth at time i. This table indicates the number of membership functions of each input variable. For the input combination (iv), the ANFIS model has 3, 3, 2 and 4 triangular membership functions for the inputs GW_{t-3}, GW_{t-2}, GW_{t-1} and GW_t, respectively.

The statistical performances of each ANFIS model in test period for Bondville well are given in Table 4. Comparing the ANFIS estimations with the measured data for the test stage demonstrates a high generalization capacity of the proposed model, for one-day-ahead forecasting, with relatively low error and high correlation, which exhibits a good performance of the ANFIS.

As seen from the upper part of Table 4, using only one previous water table depth (input combination (i)) gives good results for both stations. Introducing two, three and four previous water table depths improves the accuracy of ANFIS models and input combination (iv) can be regarded as the best model with R (0.994) and RMSE (0.277 m) for this well. For two-day-ahead forecasts, the general trend is as the same for one-day-ahead predictions, with relatively lower accuracy. Meanwhile, three-day-ahead predictions have the lowest accuracy, though the predictions made for this time interval are good. It is obviously understood that increasing prediction intervals affected the accuracy of forecasts to some extent: R decreased from 0.994 to 0.982 while the RMSE values increased from 0.277 to 0.483 m (all for input combination (iv)). Figure 5 displays the measured and predicted water table values of Bondville via scatter plots (Shiri & Kisi 2011). The figure represents the good ability of ANFIS technique for predicting the one-day-, two-day- and three-day-ahead water table depths.

The predictions for Perry well seem to be in a different trend to those of Bondville. The lower part of Table 4 gives the statistical measures of ANFIS models for Perry well. The table shows that introducing only the present water table depth produces the best result for 1, 2 and 3 day prediction intervals and increasing the input vectors results in decreasing the model accuracy for all intervals. Similar to the Bondville, increasing prediction intervals from 1 day to 3 days leads to detraction of model accuracy to some extent: R decreases from 0.991 to 0.977 and RMSE increases from 0.842 to 1.365 m, respectively. A comparison between measured and predicted water table depths

Table 4 | Statistical measures of ANFIS models in test period (Shiri & Kisi 2011)

	+1 day		+2 days		+3 days	
Input combinations	***R***	**RMSE (m)**	***R***	**RMSE (m)**	***R***	**RMSE (m)**
Bondville						
(i) GW_t	0.993	0.290	0.985	0.436	0.977	0.539
(ii) GW_{t-1}, GW_t	0.994	0.280	0.986	0.418	0.980	0.507
(iii) GW_{t-2}, GW_{t-1}, GW_t	0.994	0.280	0.986	0.417	0.981	0.498
(iv) GW_{t-3}, GW_{t-2}, GW_{t-1}, GW_t	0.994	0.277	0.987	0.405	0.982	0.483
(v) GW_{t-4}, GW_{t-3}, GW_{t-2}, GW_{t-1}, GW_t	0.994	0.283	0.987	0.406	0.981	0.486
Perry						
(i) GW_t	0.991	0.842	0.984	1.145	0.977	1.365
(ii) GW_{t-1}, GW_t	0.990	0.885	0.984	1.133	0.967	1.590
(iii) GW_{t-2}, GW_{t-1}, GW_t	0.976	1.418	0.973	1.488	0.966	1.682
(iv) GW_{t-3}, GW_{t-2}, GW_{t-1}, GW_t	0.745	5.754	0.745	5.724	0.752	5.565
(v) GW_{t-4}, GW_{t-3}, GW_{t-2}, GW_{t-1}, GW_t	0.961	1.836	0.898	3.123	0.742	5.752

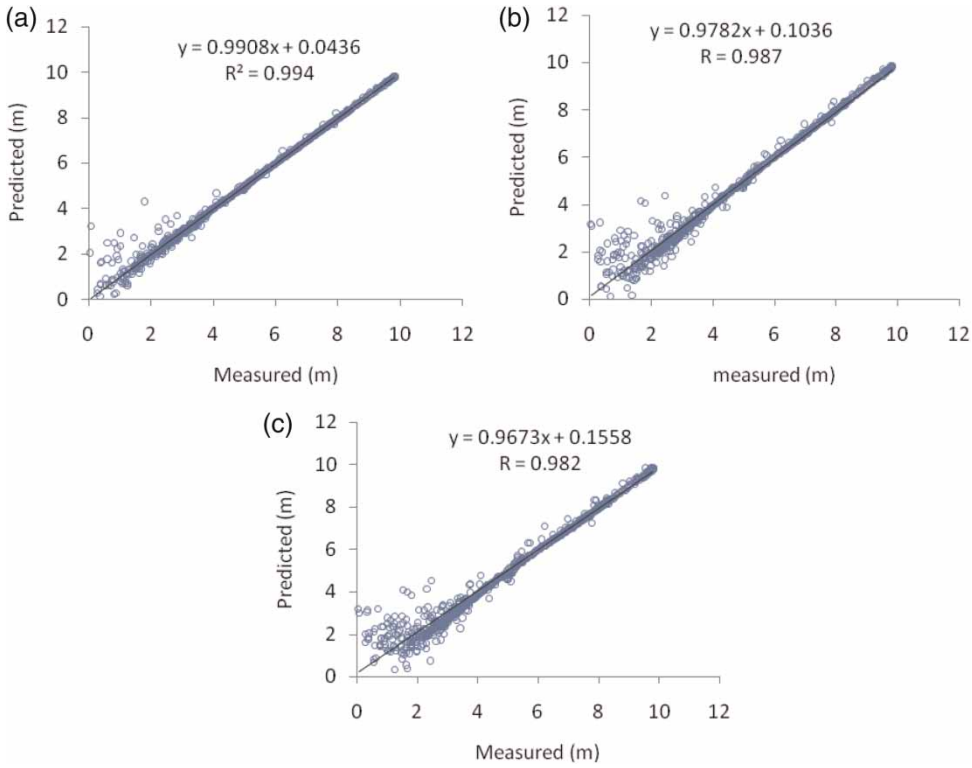

Figure 5 | Scatter plots of (a) one-day-ahead, (b) two-day-ahead and (c) three-day-ahead predictions of the best ANFIS models in Bondville well (Shiri & Kisi 2011).

is presented in Figure 6 (Shiri & Kisi 2011). From the scatter plots it is clear that the ANFIS accuracy for predicting water table depth is only good for the case ion which the present water table is introduced as a unique input. However, comparison of Figures 5 and 6 demonstrates the high accuracy of ANFIS to forecast water table depth in Bondville. The reason behind this may be the fact that the standard deviation and skewness of Perry data are relatively higher than those of the Bondville (see S_d and C_{sx} values in Table 1).

In the second step, the Wavelet-ANFIS conjunction model was evaluated to forecast groundwater table depth in both Bondville and Perry wells. As mentioned in the previous section, the data were divided into training and testing periods and five new wavelet-neuro-fuzzy models were evaluated for forecasting groundwater table depth. Table 5 represents the statistical performance of new hybrid models in terms of R and RMSE, for both Bondville (upper part of the table) and Perry (lower part of the table) wells. In the table DW_i denotes the discrete wavelet component at time i. The table clearly demonstrates the high capability of hybrid model to forecast water table depth fluctuations. For both wells, application of current day water table depth as unique model input for predicting following one-, two- and three-day-ahead depth values, gives the poor accuracy among others; however, their results are quite acceptable. Increasing previous water table depths to input combinations improves the performance of the models as follows:

(1) in the case of predicting the following one day, the model whose inputs are the current water table depth, as well as one, two, three and four previous water table depths, gives the most accurate results in terms of R (0.994–0.994) and RMSE (0.282–0.706 m) for the Bondville and Perry wells, respectively,
(2) the performance of the models are monotonously changes from R (0.985–0.984) and RMSE (0.436–1.145 m) to R (0.993–0.992) and RMSE (0.295–0.821 m) for the two-day-ahead prediction models,
(3) the statistical measures offer visible changes in case of predicting water table depths for the following three days in such a way that R increases from 0.977–0.977

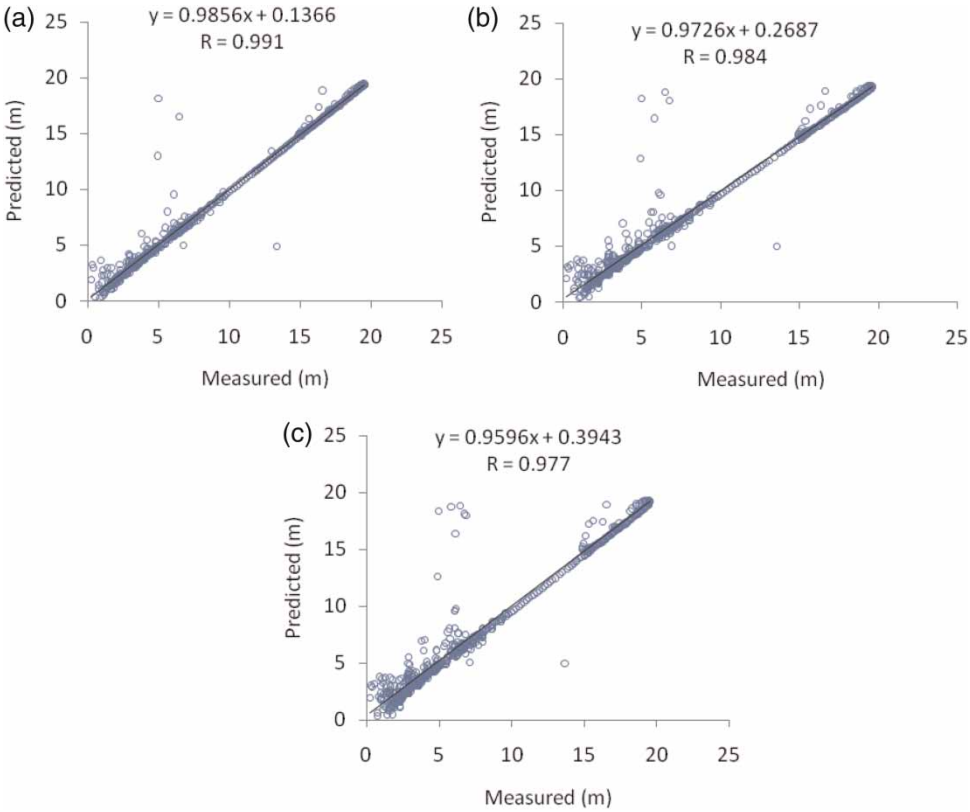

Figure 6 | Scatter plots of (a) one-day-ahead, (b) two-day-ahead and (c) three-day-ahead predictions of the best ANFIS models in Perry well (Shiri & Kisi 2011).

Table 5 | Statistical measures of wavelet-neuro-fuzzy models in the test period

Input combinations	+1 day *R*	RMSE (m)	+2 days *R*	*R*	+3 days RMSE (m)	*R*
Bondville						
(i) DW_t	0.992	0.318	0.985	0.436	0.977	0.538
(ii) DW_{t-1}, DW_t	0.993	0.295	0.987	0.398	0.982	0.482
(iii) DW_{t-2}, DW_{t-1}, DW_t	0.993	0.295	0.992	0.307	0.991	0.334
(iv) DW_{t-3}, DW_{t-2}, DW_{t-1}, DW_t	0.993	0.295	0.993	0.295	0.993	0.302
(v) DW_{t-4}, DW_{t-3}, DW_{t-2}, DW_{t-1}, DW_t	0.994	0.282	0.993	0.295	0.993	0.294
Perry						
(i) DW_t	0.992	0.975	0.984	1.145	0.977	1.365
(ii) DW_{t-1}, DW_t	0.992	0.895	0.986	1.115	0.985	1.039
(iii) DW_{t-2}, DW_{t-1}, DW_t	0.992	0.787	0.986	1.095	0.988	1.009
(iv) DW_{t-3}, DW_{t-2}, DW_{t-1}, DW_t	0.993	0.739	0.990	0.895	0.988	1.004
(v) DW_{t-4}, DW_{t-3}, DW_{t-2}, DW_{t-1}, DW_t	0.994	0.706	0.992	0.821	0.992	0.795

to 0.993–0.992 and RMSE decreases from 0.538–1.365 m to 0.294–0.795 m for the Bondville and Perry wells, respectively.

For all prediction intervals, the input combination (v) which has the highest *R* and lowest RMSE and SI values is considered as the best model for the Bondville and

Perry wells. On the other hand, comparing the hybrid model based on the input combination (v) for three predicting time intervals reveals the fact that increasing lead times has no visible effect on the model accuracies which is not the same in single ANFIS models. So, one may concluded that conjunction of wavelet and neuro-fuzzy model improves the ANFIS results. For one-day-ahead prediction, the statistical criteria of the neuro-fuzzy and hybrid models are same to each other, to some extent. In case of two-day-ahead forecasts, while the R values corresponding to input combination (v) are 0.987–0.898 for the ANFIS model, with wavelet-neuro-fuzzy model this increased to 0.993–0.992 for Bondville and Perry and the other criterion changes in descent manner as can be seen in Tables 4 and 5. Also, R values of this input combination for three-day-ahead forecasts increases from 0.981–0.742 to 0.993–0.992 and RMSE from 0.486–5.752 m to 0.294–0.795 m when applying the wavelet-neuro-fuzzy model. Figures 7 and 8 display the measured and predicted values of optimal hybrid models in Bondville and Perry wells, respectively. The figures clearly demonstrate the ability of wavelet-neuro-fuzzy model to learn the nonlinear relationship between inputs and outputs. Figures 5–8 indicate that the wavelet-neuro-fuzzy model performs better than the single neuro-fuzzy model especially for the two- and three-day-ahead forecasting of groundwater depth fluctuations. In all the (one-, two- and three-day ahead) prediction cases, the fit line equations (assume that the equation is $y = a_o x + a_1$) in the scatterplots indicate that the a_o and a_1 coefficients for the wavelet-neuro-fuzzy models are respectively closer to the 1 and 0 than those of the single neuro-fuzzy models for the Bondville and Perry wells.

Overall, the wavelet-neuro-fuzzy models that are improved combining two methods, DWT and neuro-fuzzy seem to be more adequate than the single neuro-fuzzy models for forecasting short-term groundwater depths. The complex hydrological time-series are decomposed into several simple time series using a DWT. Thus, some features

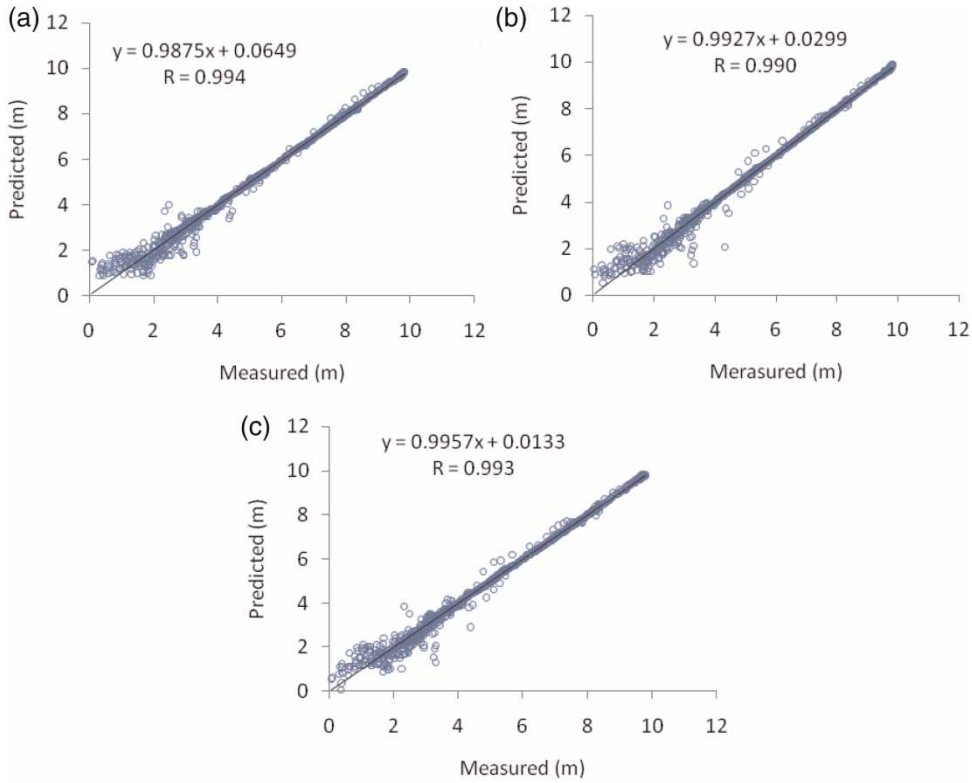

Figure 7 | Scatter plots of (a) one-day-ahead, (b) two-day-ahead and (c) three-day-ahead predictions of the best Wavelet–ANFIS models in Bondville well.

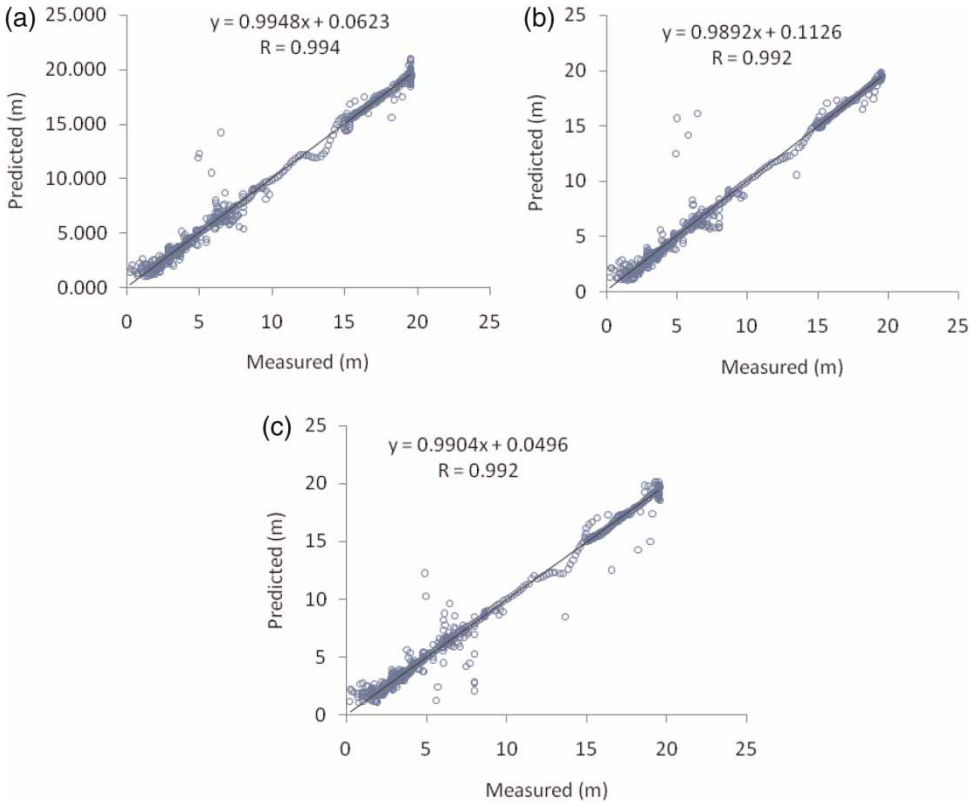

Figure 8 | Scatter plots of (a) one-day-ahead, (b) two-day-ahead and (c) three-day-ahead predictions of the best Wavelet–ANFIS models in Perry well.

of the sub-series such as its daily period can be seen more clearly than the original signal. Setting up a wavelet-neuro-fuzzy model, the neuro-fuzzy model is constructed with appropriate sub-series to belong to different scales. Forecasts are more accurate than that obtained directly by original signals because the features (such as periodically) of the sub-series are obvious, (Ning & Yunping 1998). This is why the wavelet-neuro-fuzzy model performs better than the single neuro-fuzzy model.

CONCLUSIONS

The accuracy of the wavelet-neuro-fuzzy technique in forecasting short-term (one-, two- and three-day-ahead) groundwater depth has been investigated in the present study. The groundwater depth data were decomposed into several simple time series using a DWT and the effective sub-series were used as input to the neuro-fuzzy model. It was found that excluding the detail coefficients from the inputs and using only approximation components significantly increase the accuracy of neuro-fuzzy models. The wavelet-neuro-fuzzy models were tested by applying them to the different input combinations of daily groundwater depth data of two wells, Bondville and Perry, obtained from the US Illinois State Water Survey, and the results were compared with those of the single neuro-fuzzy model. Comparison results indicated that the wavelet-neuro-fuzzy technique performs better than the neuro-fuzzy technique, especially in two- and three-day-ahead groundwater depth forecasting. In the two-day-ahead forecasting case, the wavelet-neuro-fuzzy conjunction model reduced the RMSEs with respect to the single neuro-fuzzy model by 27% (and 74%) for the Bondville and Perry wells, respectively. In the three-day ahead forecasting case, the RMSEs were reduced by 40% (respectively 86%) using the conjunction model compared with the single neuro-fuzzy model. It can thus be said that the wavelet-neuro-

fuzzy model provides a superior alternative to the neuro-fuzzy model for developing input–output simulations and forecasting short-term groundwater depths.

REFERENCES

ASCE Task Committee on Application of Artificial Neural Networks in Hydrology 2000a Artificial neural networks in hydrology. I: preliminary concepts. *J. Hydrol. Engng ASCE* **5** (2), 115–123.

ASCE Task Committee on Application of Artificial Neural Networks in Hydrology 2000b Artificial neural networks in hydrology. I: Hydrologic applications. *J. Hydrol. Engng. ASCE* **5** (2), 124–137.

Aytek, A. 2009 Co-active neurofuzzy inference system for evapotranspiration modeling. *Soft Comput.* **13**, 691–700

Beaudeau, P., Leboulanger, T., Lacroix, M., Hanneton, S. & Wang, H. Q. 2001 Forecasting of turbid floods in a coastal, chalk karstic drain using an artificial neural network. *Ground Water* **39** (1), 109–118.

Bierkens, M. F. P. 1998 Modeling water table fluctuations by means of a stochastic differential equation. *Water Resour. Res.* **34** (10), 2485–24499.

Bowden, G. J., Maier, H. R. & Dandy, G. C. 2005 Input determination for neural network models in water resourc es applications. Part1- Background and methodologies. *J. Hydrol.* **301**, 75–92.

Box, G. E. P. & Jenkins, G. M. 1976 *Time Series Analysis: Forecasting and Control*. Holden Day, Boca Raton, FL.

Cancelliere, A., Giusiano, G., Ancarani, A. & Rossi, G. 2002 A neural networks for deriving irrigation reservoir operating rules. *Water Resour. Manage.* **16**, 71–88.

Coppola, E., McLane, C., Poulton, M., Szidarovszky, F. & Magelky, R. 2005a Predicting conductance due to upconing using neural networks. *Ground Water* **43** (6), 827–836.

Coppola, E., Rana, A., Poulton, M., Szidarovszky, F. & Uhl, V. 2005b A neural network model for predicting aquifer water level elevations. *Ground Water* **43** (2), 231–241.

Coppola, E., Szidarovszky, F., Davis, D., Spayad, S., Poulton, M. & Roman, E. 2007 Multi objective analysis of a public wellfield using artificial neural networks. *Ground Water* **45** (1), 53–61.

Coulibaly, P., Anctil, F., Aravena, R. & Bobee, B. 2001 Artificial neural network modeling of water table depth fluctuations. *Water Resour. Res.* **37** (4), 885–896.

Coulibaly, P. & Burn, H. D. 2004 Wavelet analysis of variability in annual Canadian streamflows. *Water Resour. Res.* **40**, W03105.

Deka, P. & Chandramouli, V. 2003 A fuzzy neural network model for deriving the river stage-discharge relationship. *Hydrol. Sci. J.* **48** (2), 197–209.

Feng, S., Kang, S., Huo, Z., Chen, S. & Mao, X. 2008 Neural networks to simulate regional groundwater levels affected by human activities. *Ground Water* **46** (1), 80–90.

Hipel, K. W. & McLeod, A. I. 1994 *Time Series Modeling of Water Resources and Environmental Systems*. Developments in Water Science, Vol. 45, Elsevier, New York.

Jang, J. S. R. 1993 ANFIS: Adaptive-network-based fuzzy inference system. *IEEE Trans. Syst. Manage. Cybernet.* **23** (3), 665–685.

Jang, J. S. R. & Sun, C. T. 1995 Neuro fuzzy modeling and control. *Proc. IEEE* **83**, 378–405.

Jang, J. S. R., Sun, C. T. & Mizutani, E. 1997 *Neurofuzzy and Soft Computing: A Computational Approach to Learning and Machine Intelligence*. Prentice-Hall, Englewood Cliffs, NJ.

Jin, Y., Jiang, J. & Zhu, J. 1995 Neural network based fuzzy identification and its applications to modeling and control of complex systems. *IEEE Trans. Syst. Manage. Cybernet.* **25** (6), 990–997.

Kisi, O. 2005 Suspended sediment estimation using neuro-fuzzy and neural network approaches. *Hydrol. Sci. J.* **50** (4), 683–696.

Kisi, O. 2006a Generalized regression neural networks for evapotranspiration modeling. *Hydrol Sci. J.* **51** (6), 1092–1105.

Kisi, O. 2006b Evapotranspiration estimation using feed forward neural networks. *Nordic Hydrol.* **37** (3), 247–260.

Kisi, O. 2006c Daily pan evaporation modeling using a neuro-fuzzy computing technique. *J. Hydrol.* **329**, 636–646.

Kisi, O. 2007 Evapotranspiration modeling from climate data using a neural computing technique. *Hydrol. Process.* **21** (6), 1925–1934.

Kisi, O. 2009 Wavelet regression model as an alternative to neural networks for monthly streamflow forecasting. *Hydrol. Process.* **23** (25), 3583–3597.

Kisi, O. & Ozturk, O. 2007 Adaptive neurofuzzy computing technique for evapotranspiration estimation. *J. Irrig. Drain. Engng ASCE* **133** (4), 368–379.

Knotters, M. & De Gooijer, J. G. 1999 TARSO modeling of water table depths. *Water Resour. Res.* **35** (3), 695–705.

Knotters, M. & Van Walsum, P. E. V. 1997 Estimating fluctuation quantities from time series of water table depths using models with a stochastic component. *J. Hydrol.* **197**, 25–46.

Kumar, M., Raghuwanshi, N. S., Singh, R., Wallender, W. W. & Pruitt, W. O. 2002 Estimating evapotranspiration using artificial neural networks. *ASCE J. Irrig. Drain. Engng* **128** (4), 224–233.

Labat, D. 2005 Recent advances in wavelet analyses: Part 1. A review of concepts. *J. Hydrol.* **314** (1–4), 275–288.

Labat, D., Ronchail, J. & Guyot, J. L. 2005 Recent advances in wavelet analyses: Part 2–Amazon, Parana, Orinoco and Congo discharges time scale variability. *J. Hydrol.* **314** (1–4), 289–311.

Lu, R. Y. 2002 Decomposition of interdecadal and interannual components for North China rainfall in rainy season. *Chin. J. Atmos.* **26**, 611–624 (in Chinese).

Maier, H. R. & Dany, G. C. 2000 Neural networks for the prediction and forecasting of water resources variables: A review of modeling issues and applications. *Env. Model. Softw.* **15**, 101–124.

Mallat, S. G. 1989 A theory for multi resolution signal decomposition: the wavelet representation. *IEEE Trans. Pattern Anal. Machine Intell.* **11** (7), 674–693.

Mamdani, E. H. & Assilian, S. 1975 An experiment in linguistic synthesis with a fuzzy logic controller. *Int. J. Man Mach. Stud.* **7** (1), 1–13.

Milne, A. E., Macleod, C. J. A., Haygarth, P. M., Hawkins, J. M. B. & Lark, R. M. 2009 The wavelet packet transform: A technique for investigating temporal variation of river water solutes. *J. Hydrol.* **379** (1–2), 1–19.

Minns, A. W. & Hall, M. J. 1996 Artificial neural networks as rainfall-runoff models. *Hydrol. Sci. J.* **41** (3), 399–418.

Moghaddamnia, A., Ghafari Gousheh, M., Piri, J., Amin, S. & Han, D. 2009 Evaporation estimation using artificial neural networks and adaptive neurofuzzy inference system techniques. *Adv. Water Resour.* **32**, 88–97.

Mukhopadhyay, A. 1999 Spatial estimation of transmissivity using artificial neural network. *Ground Water* **37** (3), 458–464.

Ning, M. & Yunping, C. 1998 An ANN and wavelet transformation based method for short term load forecast. Energy management and power delivery. In *Proceedings of Energy Management and Power Delivery*, Vol. 2, pp. 405–410.

Palit, A. K. & Popovic, D. 1999 Forecasting chaotic time series using neuro fuzzy approach. In *Proc. IEEE IJCNN*, Washington, DC, Vol. 3, pp. 1538–1543.

Palit, A. K. & Popovic, D. 2000 Intelligent processing of time series using neuro fuzzy genetic approach. In *Proc. IEEE-ICIT Conference*, Goa, India, Vol. 1, pp. 141–146.

Palit, A. K. & Popovic, D. 2005 *Computational Intelligence in Time Series Forecasting; Theory and Engineering Applications*. Springer, Heidelberg.

Partal, T. & Kisi, O. 2007 Wavelet and neuro-fuzzy conjunction model for precipitation forecasting. *J. Hydrol.* **342**, 199–212.

Partal, T. & Küçük, M. 2006 Long-term trend analysis using discrete wavelet components of annual precipitations measurements in Marmara region (Turkey). *Phys. Chem. Earth* **31**, 1189–1200.

Shiri, J. & Kisi, O. 2010 Short-term and long-term streamflow forecasting using a wavelet and neuro-fuzzy conjunction model. *J. Hydrol.* **394** (3–4), 486–493.

Shiri, J. & Kisi, O. 2011 Comparison of genetic programming with neuro-fuzzy systems for predicting short-term water table depth fluctuations. *Comput. Geosci.*

Smith, L. C., Turcotte, D. L. & Isacks, B. 1998 Stream flow characterization and feature detection using a discrete wavelet transform. *Hydrol. Process.* **12**, 233–249.

Supharatid, S. 2003 Application of a neural network model in establishing a stage-discharge relationship for a tidal river. *Hydrol. Process.* **17**, 3085–3099.

Szidarovszky, F., Coppola, E., Long, J., Hall, A. & Poulton, M. 2007 A hybrid artificial neural network-numerical model for groundwater problems. *Ground Water* **45** (5), 590–600.

Takagi, T. & Sugeno, M. 1985 Fuzzy identification of systems and its application to modeling and control. *IEEE Trans. Syst. Manage. Cybernet.* **15** (1), 116–132.

Tankersley, C. D., Graham, W. D. & Hatfield, K. 1993 Comparison of univariate and transfer function models of groundwater fluctuations. *Water Resour. Res.* **29** (10), 2517–3533.

Tayfur, G. 2002 Artificial neural networks for sheet sediment transport. *Hydrol. Sci. J.* **4** (6), 879–892.

Xingang, D., Ping, W. & Jifan, C. 2003 Multiscale characteristics of the rainy season rainfall and interdecadal decaying of summer monsoon in North China. *Chin. Sci. Bull.* **48**, 2730–2734.

Wang, W. & Ding, J. 2003 Wavelet network model and its application to the prediction of the hydrology. *Nat. Sci.* **1** (1), 67–71.

Wang, W., Jin, J. & Li, Y. 2009 Prediction of inflow at three gorges dam in yangtze river with wavelet network model. *Water Resour. Manage.* **23**, 2791–2803.

Van Geer, F. C. & Zuur, A. F. 1997 An extension of Box-Jenkins transfer/noise models for spatial interpolation of groundwater head series. *J. Hydrol.* **192**, 65–80.

Vernieuwe, H., Georgieva, O., De Baets, B., Pauwels, V. R. N., Verhoest, N. E. C. & De Troch, F. P. 2005 Comparison of data-driven Takagi–Sugeno models of rainfall–discharge dynamics. *J. Hydrol.* **302** (1–4), 173–186.

Yang, Z. P., Lub, W. X., Long, Y. Q. & Lib, P. 2005 Application and comparison of two prediction models for groundwater levels: A case study in Western Jilin Province, China. *J. Arid Env.* **73** (4–5), 487–492.

Zhou, H. C., Peng, Y. & Liang, G-H. 2008 The research of monthly discharge predictor–corrector model based on wavelet decomposition. *Water Resour. Manage.* **22** (2), 217–227.

First received 28 October 2010; accepted in revised form 11 January 2011